

“This work has been submitted to the IEEE for possible publication. Copyright may be transferred without notice, after which this version may no longer be accessible.”

Electric Vehicle Aggregator as an Automatic Reserves Provider in the European Market Setting

I. Pavić, *Student Member, IEEE*, H. Pandžić, *Senior Member, IEEE* and T. Capuder, *Member, IEEE*

Abstract—Shift of the power system generation from the fossil to the variable renewable sources prompted the system operators to search for new sources of flexibility, that is, new reserve providers. With the introduction of electric vehicles, smart charging emerged as one of the relevant solutions. However, electric vehicle aggregators face the uncertainty of reserve activation on one side and electric vehicle availability on the other. These uncertainty can have a negative effect on both the aggregators' profitability and their users' comfort.

State-of-the art literature mostly neglects the reserve activation or the related uncertainty. Also, they rarely model European markets or use real balancing data. This paper introduces a new method for modeling the reserve activation uncertainty based on actual data for the European power system. Three electric vehicle scheduling models were designed and tested: the deterministic, the stochastic and the robust one. The results demonstrate that the current deterministic approaches inaccurately represent the activation uncertainty and that the proposed models that consider uncertainty, both the stochastic and the robust one, substantially improve the results.

Index Terms—Electric Vehicles, Electric Vehicle Aggregator, Frequency Containment Reserve, Frequency Restoration Reserve, Uncertainty

I. INTRODUCTION

Electrification of the transport sector is underway and electric vehicles (EVs) are rapidly increasing their market share [1]. Large EV fleets can have an adverse effect on the overall power system if inadequately controlled, e.g. increasing the peak power and the balancing needs. The conventional power system operation is already affected by the heavy penetration of renewable energy sources and decommissioning of fossil power plants. Thus, it is in the need of new flexibility sources that can efficiently balance the system. Smart EV charging seems to be a promising solution due to the EVs' high storage capability [2] and availability during the day [3].

Balancing in the European power systems is based on four types of reserves [4]: Frequency Containment (FCR), automatic (aFRR) and manual (mFRR) Frequency Restoration, and Replacement Reserve (RR). The FCR and aFRR are automatically activated reserves (activated upon frequency deviation and automatic generation control (AGC) signal, respectively) with fast response and short but more frequent activation events. Generally, there are two value streams when it comes to reserves, the capacity reservation and the activation fees. The reservation fee is paid for the availability of a unit to change its operating point, whereas the activation fee is paid for the actual delivery of that change [5]. Similar to stationary batteries [6], EVs are technically better suited for automatic

reserves [7] and providing them can yield high revenues [8]. Therefore, the rest of the paper exclusively focuses on FCR and aFRR.

Three sources of uncertainty can be linked to the EV energy and reserve provision algorithms: EVs' driving behaviour, prices and reserve activation (RA). Uncertainty on the EV behaviour negatively affects the EVs' availability to provide the planned services and the EV batteries' state-of-energy (SOE). This is usually modelled using behavior scenarios [9], [10], [11], [12] and often includes the second stage re-dispatching measures [13], [14], [15], [16]. The second uncertainty stream are price uncertainties that are commonly addressed through price-taker models using price scenarios [9], [11], [12], [10] or robust models where prices are determined as a worst-case scenario for the market participant [19], [20]. Another approach are the price-maker models where the bidding process is designed and the price evolves within the model itself. In such models the participants are paid on the pay-as-bid basis [15], [17] or by the market clearing price [18].

The EV behavior and price uncertainties are, in general, well supported by a recent literature. However, there is a gap in the literature in addressing the RA uncertainty. Deterministic modeling of RA [12], [13], [16], [20], [21] can create problems to EV users as well as to their aggregators [22]. The EV users may suffer from a lower SOE than required for their next trip if the activated up reserve volume was higher than anticipated. An insufficient SOE translates into a decreased comfort level for the EVs users and affects their willingness to participate in reserve provision [10]. On the other hand, if the EV drivers' needs are prioritized, the aggregators may suffer from insufficient energy volumes to back up their day-ahead (DA) plans. Aggregators may experience issues in the opposite direction as well. If down reserve is more frequently activated, the EVs' SOE will be higher than expected and they will not be able to follow their DA schedule. Inability to adhere to the agreed DA schedule causes additional balancing costs [4], whereas the inability to activate the scheduled reserve leads to penalization [16], [21], [23] and eventually disqualification from the reserve market participation [15]. The RA uncertainty modeling is thus essential for adequate reserve market participation. One of the possible approaches is stochastic modeling of the RA, as pursued in [9], [10], [12], [23]. However, the randomly generated RA scenarios, instead of the ones based on actual operation data, may not appropriately address the RA uncertainty [9], [10], [23]. On the other hand, employment of publicly available data such as AGC signals (USA-style market [12]) or RA data from the European platforms (e.g. ENTSO-E [17]) as scenarios is more

The authors are with the University of Zagreb Faculty of Electrical Engineering and Computing (e-mails: ivan.pavic@fer.hr; hrvoje.pandzic@fer.hr; tomlav.capuder@fer.hr).

appropriate. Following this reasoning, the stochastic model in this paper is designed to utilize such data.

Robust formulation of uncertainty is another approach rarely used when considering the RA and, to the best of the authors knowledge, only paper [20] pursues this idea. It considers RA as two values: the number of RA during the day (an integer value) accompanied with a binary value for each call indicating whether the reserve is fully activated or not activated at all. However, such modelling approach is more adequate for manual reserves (mFRR and RR), while automatic reserves require a more rigorous formulation of the uncertainty set. Following this approach, our paper robustly designs the RA uncertainty of the automatic reserves.

In this paper we model two types of reserves (FCR and aFRR) simultaneously and perform a comparison between their scheduling. Contrary to the majority of the papers that tackle only the USA-style markets, we focus on modeling the uncertainty of automatic RA for an EV aggregator based on real data stemming from European-style markets. Although European markets were already investigated in [15], [16], [17], none of them modeled two types of automatic reserves and none of them based the uncertainty modeling on publicly available RA data. Additionally, this paper for the first time models and compares the RA uncertainty using the stochastic and the robust approach. The contributions of the paper are thus summarized as follows:

- 1) it develops models for aFRR and FCR RA as uncertainty sets (US) based on the information from actual historic reserve data,
- 2) it integrates a newly created US of aFRR and FCR RA in an EV model and casts it as stochastic and robust linear programs,
- 3) it simulates a simultaneous provision of aFRR, FCR and DA energy and proves the efficiency and adequacy of the designed models as compared to the deterministic RA model.

The rest of the paper is organized as follows. The mathematical background is formulated and elaborated in Section II, case studies and results are presented in Section III, while Section V points out the most important findings and concludes the paper.

II. MATHEMATICAL FORMULATION

We design three models to tackle the RA uncertainty: the deterministic, the stochastic and the robust one. After presenting the nomenclature, first we develop the deterministic model, which is later used as a baseline for the stochastic and the robust counterparts.

A. Nomenclature

1) Sets and Indices:

- \mathcal{S} Set of scenarios, indexed by $s \in \{1, N_s\}$,
 \mathcal{T} Set of time steps, indexed by $t \in \{1, N_t\}$,
 \mathcal{V} Set of vehicles, indexed by $v \in \{1, N_v\}$.

2) Input Parameters:

- Δ Duration of a time-step [h],
 Λ Maximum duration of the RA,
 $A_{\{UP/DN\}-\{FCR/aFRR\}}$ Fixed up/down FCR/aFRR RA ratio,
 C_v^B Capital battery cost of EV v [€],

- $C_{v,t}^{FCH}$ Fast charging fee [€/kWh],
 C_t^{DA} Day-ahead market electricity price [€/kWh],
 B_v Battery capacity of EV v [kWh],
 $CA_t^{\{UP/DN\}-\{FCR/aFRR\}}$ Reserve activation fee [€/kWh],
 $CR_t^{\{UP/DN\}-\{FCR/aFRR\}}$ Reserve capacity fee [€/kWh/Δ],
 $D_{\{1/2/3/4\}}^B$ Battery degradation coefficients,
 $E_{v,t}^{RUN}$ Energy used for driving of EV v [kWh],
 $P_{v,t}^{CP_MAX}$ Charging point maximum power limit [kW],
 $P_{v,t}^{FCH_MAX}$ Maximum power limit for fast charging [kW],
 $P_{v,t}^{OBC_MAX}$ Maximum OBC power limit for EV v [kW],
 $SOE_v^{\{MIN/MAX\}}$ Minimum/maximum SOE of EV v [%],
 SOE_v^{T0} Initial SOE of EV v [%],
 $\eta^{\{RUN/V2G\}}$ EV driving/V2G discharging efficiency,
 $\eta^{\{FCH/SCH\}}$ EV fast/slow charging efficiency.

3) Variables:

- c^{OTH} Aggregator costs aside from reserve activation [€],
 c^{ACT} Aggregator costs arising from reserve activation [€],
 $c_{v,t}^{DEG}$ Degradation cost attributed to EV v [€],
 $e_{v,t}^{\{BUY/SELL\}-DA}$ Energy traded in the DA market [kWh],
 $e_{v,t}^{DCH}$ Energy discharged from EV v [kWh],
 $e_{v,t}^{\{FCH/SCH\}}$ Energy fast/slow-charged to EV v [kWh],
 $e_{v,t}^{DEG}$ Energy used for degradation [kWh],
 $e_{v,t}^{OTH}$ Accumulated en. other than from RA [MWh],
 $e_{v,t}^{ACT}$ Accumulated energy from reserve RA [MWh],
 $r_{v,t}^{\{UP/DN\}-\{FCR/aFRR\}}$ Reserve capacity sold in reserve markets,
 $soe_{v,t}^{EV}$ State-of-energy of EV v [kWh].

B. Deterministic Model – DM

The RA is usually modeled as an annual average of activations, e.g. [12], [13], [16], [20], [21]. Similarly, the deterministic model (DM) in this paper, which we use as a baseline, is based on the average annual RA ratio of a particular reserve product. Therefore, the RA ratio the same at all timesteps. The objective function (OF) includes five parts: cost/revenue from energy traded in the DA market, revenue from power sold as FCR/aFRR capacity, V2G battery degradation cost, fast-charging cost and cost/revenue from energy withdrawn/injected as the activated FCR/aFRR. The first four costs other than from RA are assigned to c^{OTH} defined in eq. (D-2), while the costs associated to RA are assigned to c^{ACT} defined in eq. (D-3). Objective function:

$$\min_{\Xi_{\mathcal{O}}} (c^{OTH} + c^{ACT}); \quad (D-1)$$

is subject to:

$$c^{OTH} = \sum_{t=1}^{N_t} \left\{ \sum_{v=1}^{N_v} [e_{v,t}^{BUY_DA} \cdot C_t^{DA} - e_{v,t}^{SELL_DA} \cdot C_t^{DA} - r_{v,t}^{UP_FCR} \cdot CR_t^{UP_FCR} - r_{v,t}^{DN_FCR} \cdot CR_t^{DN_FCR} - r_{v,t}^{UP_aFRR} \cdot CR_t^{UP_aFRR} - r_{v,t}^{DN_aFRR} \cdot CR_t^{DN_aFRR} + c_{v,t}^{DEG} + e_{v,t}^{FCH} \cdot C_{v,t}^{FCH}] \right\}; \quad (D-2)$$

$$c^{ACT} = \sum_{t=1}^{N_t} \left\{ \sum_{v=1}^{N_v} [-r_{v,t}^{UP_FCR} \cdot A_{UP_FCR} \cdot \Delta \cdot CA_t^{UP_FCR} + r_{v,t}^{DN_FCR} \cdot A_{DN_FCR} \cdot \Delta \cdot CA_t^{DN_FCR} - r_{v,t}^{UP_aFRR} \cdot A_{UP_aFRR} \cdot \Delta \cdot CA_t^{UP_aFRR} + r_{v,t}^{DN_aFRR} \cdot A_{DN_aFRR} \cdot \Delta \cdot CA_t^{DN_aFRR}] \right\}; \quad (D-3)$$

$$e_{v,t}^{\text{BUY_DA}}, e_{v,t}^{\text{SELL_DA}}, r_{v,t}^{\text{UP_FCR}}, r_{v,t}^{\text{DN_FCR}}, r_{v,t}^{\text{UP_aFRR}}, r_{v,t}^{\text{DN_aFRR}} \geq 0; \quad (\text{D-4})$$

$$e_{v,t}^{\text{SELL_DA}}/\Delta - e_{v,t}^{\text{BUY_DA}}/\Delta + r_{v,t}^{\text{UP_FCR}} + r_{v,t}^{\text{UP_aFRR}} \leq \min(P_v^{\text{OBC_MAX}}, P_{v,t}^{\text{CP_MAX}}); \quad (\text{D-5})$$

$$e_{v,t}^{\text{BUY_DA}}/\Delta - e_{v,t}^{\text{SELL_DA}}/\Delta + r_{v,t}^{\text{DN_FCR}} + r_{v,t}^{\text{DN_aFRR}} \leq \min(P_v^{\text{OBC_MAX}}, P_{v,t}^{\text{CP_MAX}}); \quad (\text{D-6})$$

$$soe_{v,t}^{\text{EV}} = SOE^{\text{T0}} \cdot B_v + e_{v,t}^{\text{OTH}} + e_{v,t}^{\text{ACT}}; \quad (\text{D-7})$$

$$e_{v,t}^{\text{OTH}} = \sum_{\tau=1}^t \{ e_{v,\tau}^{\text{BUY_DA}} \cdot \eta^{\text{CH}} - e_{v,\tau}^{\text{SELL_DA}}/\eta^{\text{DCH}} - E_{v,\tau}^{\text{RUN}}/\eta^{\text{RUN}} + e_{v,\tau}^{\text{FCH}} \cdot \eta^{\text{FCH}} \}; \quad (\text{D-8})$$

$$e_{v,t}^{\text{ACT}} = \sum_{\tau=1}^t \left\{ \Delta \cdot [\eta^{\text{CH}} \cdot (r_{v,\tau}^{\text{DN_FCR}} \cdot A^{\text{DN_FCR}} + r_{v,\tau}^{\text{DN_aFRR}} \cdot A^{\text{DN_aFRR}}) - 1/\eta^{\text{DCH}} \cdot (r_{v,\tau}^{\text{UP_FCR}} \cdot A^{\text{UP_FCR}} + r_{v,\tau}^{\text{UP_aFRR}} \cdot A^{\text{UP_aFRR}})] \right\}; \quad (\text{D-9})$$

$$SOE^{\text{MIN}} \cdot B_v \leq soe_{v,t}^{\text{EV}} + e_{v,t+1}^{\text{BUY_DA}} \cdot \eta^{\text{CH}} - e_{v,t+1}^{\text{SELL_DA}}/\eta^{\text{DCH}} - \Lambda \cdot \Delta/\eta^{\text{DCH}} \cdot (r_{v,t+1}^{\text{UP_FCR}} + r_{v,t+1}^{\text{UP_aFRR}}) - E_{v,t+1}^{\text{RUN}}/\eta^{\text{RUN}} + e_{v,t+1}^{\text{FCH}} \cdot \eta^{\text{FCH}} \quad \forall t \in \mathcal{T}_{(t \neq N_t)}; \quad (\text{D-10})$$

$$SOE^{\text{MAX}} \cdot B_v \geq soe_{v,t}^{\text{EV}} + e_{v,t+1}^{\text{BUY_DA}} \cdot \eta^{\text{CH}} - e_{v,t+1}^{\text{SELL_DA}}/\eta^{\text{DCH}} + \Lambda \cdot \Delta \cdot \eta^{\text{CH}} \cdot (r_{v,t+1}^{\text{DN_FCR}} + r_{v,t+1}^{\text{DN_aFRR}}) - E_{v,t+1}^{\text{RUN}}/\eta^{\text{RUN}} + e_{v,t+1}^{\text{FCH}} \cdot \eta^{\text{FCH}} \quad \forall t \in \mathcal{T}_{(t \neq N_t)}; \quad (\text{D-11})$$

$$SOE^{\text{T0}} \cdot B_v \leq soe_{v,t}^{\text{EV}} \leq SOE^{\text{MAX}} \cdot B_v \quad \text{for } t = N_t; \quad (\text{D-12})$$

$$0 \leq e_{v,t}^{\text{FCH}} \leq P^{\text{FCH_MAX}} \cdot \Delta; \quad (\text{D-13})$$

$$e_{v,t}^{\text{DEG}} = e_{v,t}^{\text{SELL_DA}}/\eta^{\text{DCH}} - e_{v,t}^{\text{BUY_DA}} \cdot \eta^{\text{CH}} + \Delta/\eta^{\text{DCH}} \cdot (r_{v,t}^{\text{UP_FCR}} \cdot A^{\text{UP_FCR}} + r_{v,t}^{\text{UP_aFRR}} \cdot A^{\text{UP_aFRR}}) - \Delta \cdot \eta^{\text{CH}} \cdot (r_{v,t}^{\text{DN_FCR}} \cdot A^{\text{DN_FCR}} + r_{v,t}^{\text{DN_aFRR}} \cdot A^{\text{DN_aFRR}}); \quad (\text{D-14})$$

$$c_{v,t}^{\text{DEG}} \geq 0; \quad (\text{D-15})$$

$$c_{v,t}^{\text{DEG}} \cdot B_v \geq C_v^{\text{B}} \cdot [-D_1^{\text{B}} \cdot B_v + D_2^{\text{B}} \cdot e_{v,t}^{\text{DEG}} + D_3^{\text{B}} \cdot (B_v - soe_{v,t}^{\text{EV}})]; \quad (\text{D-16})$$

$$c_{v,t}^{\text{DEG}} \cdot B_v \geq C_v^{\text{B}} \cdot D_4^{\text{B}} \cdot e_{v,t}^{\text{DEG}}. \quad (\text{D-17})$$

Eq. (D-2) sums the DA market costs (consisting of energy purchase and sell as well as up and down FCR and aFRR capacity reservation), battery degradation and fast charging cost. On the other hand, eq. (D-3) contains only the RA costs, where up RA is remunerated by the system operator (hence the minus sign), while the down RA must be paid to the system operator (hence the plus sign). Eq. (D-4) sets the six market bidding variables as nonnegative. Eqs. (D-5) and (D-6) limit the total charging/discharging power available for bidding to the minimum of the On-Board Charger (OBC) capacity and the Charging Point (CP) capacity. In other words, (D-5) and (D-6) allocate the available power to the six market bidding variables appearing in these constraints.

Eq. (D-7) calculates the current SOE based on the initial SOE and the energy charged/discharged to/from the EV's battery until the time-step t . The energy can be charged/discharged by the means of DA market trading, driving, fast charging (D-8) and RA (D-9). Energy consumed for driving in one time-step originates from the input data of the EV driving/parking behaviour explained in Subsection

III-B. The amount of energy injected/extracted due to RA is modeled using parameters $A^{\{\text{UP/DN}\}_{\text{FCR/aFRR}}} \in [0, 1]$. To make sure that the EV batteries will be able to deliver the required reserves, their capacity is limited in eqs. (D-10) and (D-11) assuming a their full activation. Eq. (D-10) acts as the lower bound to the SOE, where only the full up RA is considered. Similarly, eq. (D-11) acts as the upper bound to the SOE considering the full down RA. These two equations ensure that the SOE is feasible in each time step even for the full RA. Eqs. (D-10) and (D-11) are applied up to timestep $t < N_t$. In the last timestep the conventional SOE preservation eq. (D-12) is applied. The fast-charging limit is enforced in (D-13).

Li-ion batteries are prone to degradation, especially when cycled often. Incorporating degradation cost in the OF may reduce the battery charging/discharging actions not related to driving. The degradation is taken into account when discharging in the DA market or through RA in eq. (D-14). Eq. (D-15) sets $c_{v,t}^{\text{DEG}}$ as a positive variable. Eqs. (D-16) and (D-17) bound and calculate the V2G discharging degradation cost. Those constraints are a linearized form of the degradation model from [24]. The above constraints (D-4)–(D-17) apply for $\forall v \in \mathcal{V}$ and $\forall t \in \mathcal{T}$, except for eqs. (D-10)–(D-11), which are not valid in the last period, and for (D-12), which is valid in the last period only.

C. Stochastic Model – SM

The stochastic model (SM) differs from the DM in the definition of the RA ratio. While the DM uses one value for all timesteps, the SM uses the RA ratio as a time-dependable parameter taken from the historic data using several scenarios (details on how this data is used is explained in Section III-A). The RA parameters $A_{s,t}^{\{\text{UP/DN}\}_{\text{FCR/aFRR}}}$ and the associated variables $g_s^{\text{RA}}, h_s^{\text{RA}}, soe_{s,v,t}^{\text{EV}}, e_{s,v,t}^{\text{DEG}}, c_{s,v,t}^{\text{DEG}}$ gain an additional index s . The model is accordingly reformulated using eqs. (S-1)–(S-4). The OF of the SM is (S-1). Eqs. in (S-2) are identical as in the DM, while the SM instances of eqs. (S-3) and (S-4) include additional index $\forall s \in \mathcal{S}$. Objective function:

$$\min_{\Xi_{\mathcal{O}}} [P_s \cdot \sum_{s=1}^{N_s} (c_s^{\text{OTH}} + c_s^{\text{ACT}})]; \quad (\text{S-1})$$

$$\text{subject to:} \quad (\text{D-4}) - (\text{D-6}); \quad (\text{S-2})$$

$$(\text{D-3}), (\text{D-9}), (\text{D-14}), \quad \forall s \in \mathcal{S}; \quad (\text{S-3})$$

$$(\text{D-2}), (\text{D-7}) - (\text{D-8}), (\text{D-10}) - (\text{D-13}),$$

$$(\text{D-15}) - (\text{D-17}), \quad \forall s \in \mathcal{S}. \quad (\text{S-4})$$

D. Robust Model – RM

In the robust model (RM) the RA quantities are uncertain parameters $(a_{v,\tau,t}^{\text{UP_FCR}}, a_{v,\tau,t}^{\text{DN_FCR}}, a_{v,\tau,t}^{\text{UP_aFRR}}, a_{v,\tau,t}^{\text{DN_aFRR}})$ whose boundaries are defined by the uncertainty set (US) defined in eqs. (US-1)–(US-8) with parameters resulting from the probabilistic analysis in Section III-A. OF (RI-1) of the RM minimizes the total operating costs for the worst-case RA, i.e. maximizing the RA throughout the day, (RI-4)–(RI-8). Such min-max structure cannot be solved directly and an appropriate RM reformulation presented in [28] was used.

The initial formulation of the RM is presented in Section II-D1. Using the duality theory, subproblems (RI-4)–(RI-8) are recast as duals and merged with the rest of the constraints creating the final problem presented in Section II-D2.

1) *Initial Formulation:*

Objective function:

$$\min_{\Xi_{\mathcal{O}}} (z) \quad (\text{RI-1})$$

is subject to:

$$(\text{D-2}), (\text{D-4}) - (\text{D-6}), (\text{D-8}), (\text{D-13}) - (\text{D-17}); \quad (\text{RI-2})$$

$$(\text{D-3}), (\text{D-9}); \quad (\text{RI-3})$$

$$\max_{\Xi_{\mathcal{A}}} (c^{\text{ACT}}) \leq z - c^{\text{OTH}}; \quad (\text{RI-4})$$

$$\begin{aligned} \max_{\Xi_{\mathcal{A}}} (-e_{v,t}^{\text{ACT}}) &\leq B_v \cdot (SOE^{\text{T0}} - SOE^{\text{MIN}}) \\ -\Lambda \cdot \Delta / \eta^{\text{DCH}} \cdot (r_{v,t+1}^{\text{UP_FCR}} + r_{v,t+1}^{\text{UP_aFRR}}) &+ e_{v,t+1}^{\text{OTH}}; \quad (\text{RI-5}) \\ \max_{\Xi_{\mathcal{A}}} (e_{v,t}^{\text{ACT}}) &\leq B_v \cdot (SOE^{\text{MAX}} - SOE^{\text{T0}}) \end{aligned}$$

$$-\Lambda \cdot \Delta \cdot \eta^{\text{CH}} \cdot (r_{v,t+1}^{\text{DN_FCR}} + r_{v,t+1}^{\text{DN_aFRR}}) - e_{v,t+1}^{\text{OTH}}; \quad (\text{RI-6})$$

$$\max_{\Xi_{\mathcal{A}}} (e_{v,t}^{\text{ACT}}) \leq B_v \cdot (SOE^{\text{MAX}} - SOE^{\text{T0}}) - e_{v,t}^{\text{OTH}}; \quad (\text{RI-7})$$

$$\max_{\Xi_{\mathcal{A}}} (-e_{v,t}^{\text{ACT}}) \leq e_{v,t}^{\text{OTH}}, \quad \text{for } t = N_t; \quad (\text{RI-8})$$

OF of the RM (RI-1) minimizes the total cost of an EV fleet. Eqs. (RI-2) are the same as in the DM, while the uncertain parameters are located in the constraints containing the RA variables, grouped under eq. (RI-3). Eqs. (RI-3) are similar as in the DM, but the fixed RA parameter is replaced with an uncertain one. OF and each constraint containing the terms with uncertain parameters from (RI-3) are observed as independent maximization subproblems (RI-4)–(RI-8). OF of the DM eqrefOF is reformulated to its robust counterpart presented in eqs. (RI-1) and (RI-4). Eqs. (D-10)–(D-12) bounding the SOE are adequately reformulated to eqs. (RI-5)–(RI-8).

Subproblems defined by eqs. (RI-4)–(RI-8) are valid $\forall (a_{v,\tau,t}^{\text{UP_FCR}}, a_{v,\tau,t}^{\text{DN_FCR}}, a_{v,\tau,t}^{\text{UP_aFRR}}, a_{v,\tau,t}^{\text{DN_aFRR}}) \in \mathcal{A}$, where \mathcal{A} is the following US:

$$\mathcal{A} = \{a_{v,\tau,t}^{\text{UP_FCR}}, a_{v,\tau,t}^{\text{DN_FCR}}, a_{v,\tau,t}^{\text{UP_aFRR}}, a_{v,\tau,t}^{\text{DN_aFRR}} \mid a_{v,\tau,t}^{\text{UP_FCR}}, a_{v,\tau,t}^{\text{DN_FCR}}, a_{v,\tau,t}^{\text{UP_aFRR}}, a_{v,\tau,t}^{\text{DN_aFRR}} \geq 0; \quad (\text{US-1})$$

$$a_{v,\tau,t}^{\text{UP_FCR}} + a_{v,\tau,t}^{\text{DN_FCR}} \leq A^{\text{MAX_FCR}} : \omega_{v,\tau,t}^{(\text{RI-5})_FCR}; \quad (\text{US-2})$$

$$\sum_{\tau=1}^t a_{v,\tau,t}^{\text{UP_FCR}} \leq (\Gamma^{\text{UP_FCR}} - 1) \cdot I_t + 1 : \mu_{v,t}^{(\text{RI-5})_FCR}; \quad (\text{US-3})$$

$$\sum_{\tau=1}^t a_{v,\tau,t}^{\text{UP_FCR}} \geq \Upsilon^{\text{UP_FCR}} \cdot I_t : \nu_{v,t}^{(\text{RI-5})_FCR}; \quad (\text{US-4})$$

$$\sum_{\tau=1}^t a_{v,\tau,t}^{\text{DN_FCR}} \leq (\Gamma^{\text{DN_FCR}} - 1) \cdot I_t + 1 : \psi_{v,t}^{(\text{RI-5})_FCR}; \quad (\text{US-5})$$

$$\sum_{\tau=1}^t a_{v,\tau,t}^{\text{DN_FCR}} \geq \Upsilon^{\text{DN_FCR}} \cdot I_t : \chi_{v,t}^{(\text{RI-5})_FCR}; \quad (\text{US-6})$$

$$(\text{US-2})\text{--}(\text{US-6}) \text{ are analogous for aFRR}; \quad (\text{US-7})$$

$$(\text{US-2})\text{--}(\text{US-7}) \text{ are similar for (RI-4)–(RI-8)}. \quad (\text{US-8})$$

The US presented in eqs. (US-1)–(US-6) applies to the *FCR* service and for the subproblem stated in (RI-5). The uncertainty set (US-7) spreads it over the *aFRR* service and (US-8) to other robust subproblems. For constraints (RI-5) and (RI-6) the US is applied up to a specific time-step t and for a specific EV v . The US equations, uncertain parameters and dual variables for (RI-6) are the same as for (RI-5).

The US for OF (RI-4) is applied over the entire horizon $[1, N_t]$ and entire EV fleet $[1, N_v]$, whereas in (RI-7) and (RI-8) it is applied up to the last time-step N_t (mathematically it is the same as for the (RI-4)) and for a specific EV v . Following this reasoning, index τ is omitted in the dual variables,

uncertain parameters and the summation terms in (US-3)–(US-6) (the sum goes from $t \in [1, N_t]$) for (RI-4), (RI-7) and (RI-8). For (RI-4), index v is also omitted. Therefore, for OF (RI-4) the dual variable of constraint (US-2) is indexed only with t (i.e. $\omega_t^{(\text{RI-4})}$) and the dual variables of the rest of the constraints (US-3)–(US-6) do not have an index (e.g. $\mu^{(\text{RI-4})}$). Dual variables for (RI-7) and (RI-8) are the same as for (RI-4) but they include index v (e.g. $\omega_{t,v}^{(\text{RI-8})}$, $\mu_v^{(\text{RI-8})}$).

For OF (RI-4), (RI-7)–(RI-8), parameter I_t is always equal to 1, while for constraints (RI-5)–(RI-6) it represents a uniformly distributed range $\in [0, 1]$ for index $t \in [1, N_t]$. Parameter I_t is designed to partition the min (Υ)/max (Γ) total activated reserve in time-frames shorter than N_t .

2) *Final Formulation:*

Objective function:

$$\min_{\Xi_{\mathcal{O}}} (z) \quad (\text{RF-1})$$

subject to:

$$(\text{D-2}), (\text{D-4}) - (\text{D-6}), (\text{D-8}), (\text{D-13}) - (\text{D-17}); \quad (\text{RF-2})$$

$$(\text{D-3}), (\text{D-9}); \quad (\text{RF-3})$$

$$G_t^{\{\text{UP/DN}\}\text{-}\{\text{FCR/aFRR}\}} = (\Gamma^{\{\text{UP/DN}\}\text{-}\{\text{FCR/aFRR}\}} - 1) \cdot I_{t+1} \quad (\text{RF-4})$$

$$\begin{aligned} &A^{\text{MAX_FCR}} \cdot \sum_{\tau=1}^t \omega_{v,\tau,t}^{(\text{RI-5})_FCR} \\ &+ G_t^{\text{UP_FCR}} \cdot \mu_{v,t}^{(\text{RI-5})_FCR} + \Upsilon^{\text{UP_FCR}} \cdot I_t \cdot \nu_{v,t}^{(\text{RI-5})_FCR} \\ &+ G_t^{\text{DN_FCR}} \cdot \psi_{v,t}^{(\text{RI-5})_FCR} + \Upsilon^{\text{DN_FCR}} \cdot I_t \cdot \chi_{v,t}^{(\text{RI-5})_FCR} \\ &A^{\text{MAX_aFRR}} \cdot \sum_{\tau=1}^t \omega_{v,\tau,t}^{(\text{RI-5})_aFRR} \\ &+ G_t^{\text{UP_aFRR}} \cdot \mu_{v,t}^{(\text{RI-5})_aFRR} + \Upsilon^{\text{UP_aFRR}} \cdot I_t \cdot \nu_{v,t}^{(\text{RI-5})_aFRR} \\ &+ G_t^{\text{DN_aFRR}} \cdot \psi_{v,t}^{(\text{RI-5})_aFRR} + \Upsilon^{\text{DN_aFRR}} \cdot I_t \cdot \chi_{v,t}^{(\text{RI-5})_aFRR} \\ &\leq B_v \cdot (SOE^{\text{T0}} - SOE^{\text{MIN}}) \\ &-\Lambda \cdot \Delta / \eta^{\text{DCH}} \cdot (r_{v,t+1}^{\text{UP_FCR}} + r_{v,t+1}^{\text{UP_aFRR}}) + h_{v,t+1}^{\text{NRA}}; \quad (\text{RF-5}) \end{aligned}$$

$$\omega_{v,\tau,t}^{(\text{RI-5})_FCR} + \mu_{v,t}^{(\text{RI-5})_FCR} + \nu_{v,t}^{(\text{RI-5})_FCR} \geq \Delta / \eta^{\text{DCH}} \cdot r_{v,\tau}^{\text{UP_FCR}} : a_{v,\tau,t}^{\text{UP_FCR}}; \quad (\text{RF-6})$$

$$\omega_{v,\tau,t}^{(\text{RI-5})_FCR} + \psi_{v,t}^{(\text{RI-5})_FCR} + \chi_{v,t}^{(\text{RI-5})_FCR} \geq -\Delta \cdot \eta^{\text{CH}} \cdot r_{v,\tau}^{\text{DN_FCR}} : a_{v,\tau,t}^{\text{DN_FCR}}; \quad (\text{RF-7})$$

$$\omega_{v,\tau,t}^{(\text{RI-5})_FCR}, \mu_{v,t}^{(\text{RI-5})_FCR}, \psi_{v,t}^{(\text{RI-5})_FCR} \geq 0; \quad (\text{RF-8})$$

$$\nu_{v,t}^{(\text{RI-5})_FCR}, \chi_{v,t}^{(\text{RI-5})_FCR} \leq 0; \quad (\text{RF-9})$$

$$(\text{RF-6})\text{--}(\text{RF-9}) \text{ are analogous for FRR}; \quad (\text{RF-10})$$

$$(\text{RF-4})\text{--}(\text{RF-10}) \text{ are analogous for (RI-4)–(RI-8)}. \quad (\text{RF-11})$$

Eqs. (RF-1)–(RF-3) are the same as in the RI formulation. Auxiliary eq. (RF-4) is used to shorten the notation. Eqs. (RF-5)–(RF-9) represent strong duality and dual constraints (for FCR) of the subproblem stated in (RI-5). Eq. (RF-5) applies $\forall t \in \mathcal{T}$ and $\forall v \in \mathcal{V}$, while eqs. (RF-6)–(RF-9) additionally apply $\forall \tau \in \mathcal{T}, \tau < t$. Eq. (RF-10) spreads the problem over aFRR dual constraints and eq. (RF-11) spreads it on subproblems (RI-4), (RI-6)–(RI-8). The left-hand side in eqs. (RF-5)–(RF-7) is the same for subproblem (RI-6) (only the superscript of dual variables changes), whereas for subproblems (RI-4), (RI-7) and (RI-8) the indices must be aligned to those of the US dual variables (the sum in (RF-5) goes from $t \in [1, N_t]$). Constraints for (RI-4) are simplified versions of (RF-5)–(RF-10) as they apply over all \mathcal{T} and \mathcal{V} .

Eqs. for subproblems (RI-7) and (RI-8) retain index $\forall v \in \mathcal{V}$. The right-hand sides in eqs. (RF-5)–(RF-7) must be aligned with cost coefficients on the left-hand side and limits on the right-hand side of (RI-4)–(RI-8).

III. CASE STUDIES

The developed models were deployed to obtain the DA schedules. The quality of the obtained schedules was assessed by running them against one hundred historical RA scenarios. Three models are tested: the DM with average annual RA, the SM with 10 ex-ante RA scenarios and the RM with the US based on the real balancing data.

A. Reserve Activation – RA

The core input data to calculate the RA ratios are $FCR/aFRR$ Accepted Reserve Capacity (ARC) bids and $FCR/aFRR$ Activated Reserve Energies (ARE) taken from the RTE for the year 2018 [25]. For each half-hourly period (and each reserve type and direction) the RA quantities are calculated as:

$$\left(RA_{ratio}_t = \frac{ARE_t}{ARC_t \cdot \Delta} \right)_{\{UP/DN\}_{\{FCR/aFRR\}}} \quad (A-1)$$

Using the calculated half-hourly ratios, a statistical analyses was performed to gain the required input data. Visualization of the obtained results for FCR and aFRR are presented in Figure 1. These data are used to determine the average values for the DM, to select scenarios for the SM, and to obtain inputs for the US of the RM. Also, it will be used to select RA scenarios for the ex-post validation of the models.

Probability distribution functions (PDF) for up and down reserves are very similar for both the FCR and the aFRR. The down reserve has a slightly higher annual average value for both the FCR and the aFRR. Also, average values for both UP and DN are much higher for aFRR than for FCR. The activation values used in the DM are shown in Table I in the second column. Scenarios for the SM are taken as the realized RA ratios for each reserve type and direction from Jan. 11-20, 2018 (10 in total). Ex-post validation is performed on scenarios from April 1, 2018 to July 9, 2018 (100 in total).

For the US of the RM two values are required, the maximum achieved RA ratios in each time-step and the overall daily activated energy. The RA ratios for UP and DN reserves are dependent variables where a high RA value of one direction entails a low RA value of the other direction and vice versa (valid for both the FCR and the aFRR). This statement is modeled in (US-2) and shown as green (max) and cyan (99%) lines on graphs in Figures 1a and 1b. This also bounds the individual RA ratios of the up and down reserves. The FCR RA ratio never reaches 1; the maximum value for UP RA ratio is 0.47 and for DN RA ratio 0.73. In 99% of the points the UP and DN RA ratios are lower or equal to 0.29 and 0.36, respectively. High aFRR RA ratios are also rare, but more frequent than in the case of FCR so the 99% lines in Figure 1b are at 0.96 and 1 for UP and DN RA ratios, respectively. The parameters used in the case study are shown in Table I. Those in the third column are used for subproblem (RI-4) and those in the fifth column are used for subproblems (RI-5)–(RI-8). The daily sums of the RA ratios throughout the year are always

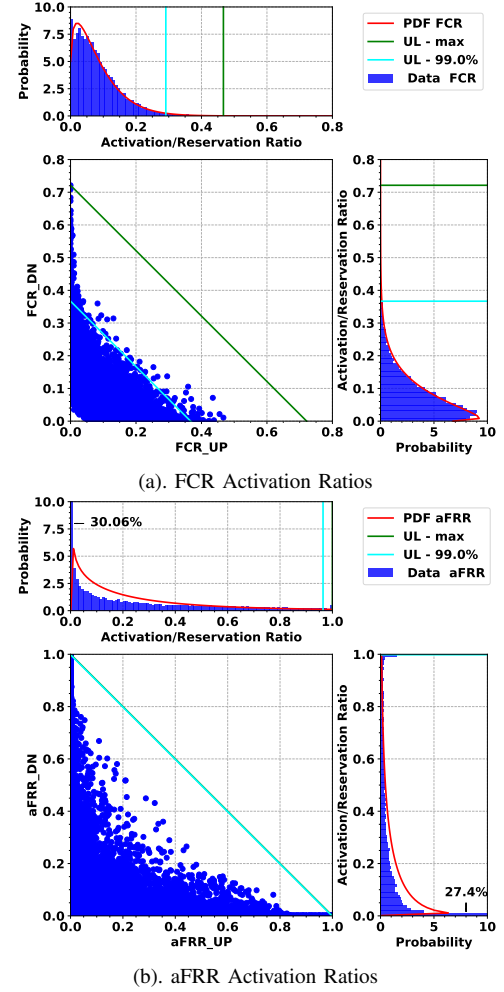


Fig. 1. Activation Ratios – Historical Data

within certain upper and lower limits, which is modeled in the US constraints (US-3)–(US-6). The median of the daily sums for each of the reserve and direction are shown in Table I in column four. This data is used as both Υ and Γ parameters for subproblem (RI-4). The minimum and maximum of the daily sums for each of the reserve and direction are shown in Table I in columns six and seven, respectively. This data is used as Υ and Γ parameters for subproblems (RI-5)–(RI-8).

B. Input Parameters

The EV driving/parking behaviour was consolidated from the JRC European driving study [3], [26], and [27]. The data was restructured to represent 5-min EV driving/parking behaviour where in each 5-min timestamp each EV can either drive or be parked. Vehicle type and average trip speed were used as inputs to calculate the EV consumption while

TABLE I
RA RATIO INPUTS FOR DM AND RM

Model	DM	RM for (RI-4)		RM for (RI-5)–(RI-8)		
Parameter	A	A^{MAX}	$\Gamma = \Upsilon$	A^{MAX}	Υ	Γ
Input	Mean	0.99%	Med	Max	Min	Max
UP_FCR	0.082	0.36	4	0.73	0.93	8.21
DN_FCR	0.085		3.8		1.10	16.64
UP_aFRR	0.198	1	9.13	1	2.10	21.31
DN_aFRR	0.218		9.70		2.62	20.51

driving. Starting/finishing trip locations were used to assign instantaneous CP capacity, i.e. to choose the CP type. Three CP types were modeled: low (3.7 kW), medium (7.4 kW) and high (11 kW). Starting/finishing trip times were used to assign whether an EV is driving or is parked. The 5-min timestamps were then summarized into half-hourly periods to match the half-hourly optimization time resolution. As a result, for each EV and each half-hourly period, two input parameters were created: EV driving consumption ($E_{v,t}^{\text{RUN}}$ in eq. (D-7)) and maximum CP power ($P_{v,t}^{\text{CP_MAX}}$ in eqs. (D-5) and (D-6)). The data-set for France was used with the total of 581 EVs divided in three types based on vehicle type (battery capacity, OBC size, fleet share): small (20 kWh, 3.7 kW, 30%), medium (40 kWh, 7.4 kW, 40%) and large (60 kWh, 11 kW, 30%). The total fleet capacity is 23.08 MWh, and the total OBC power is 4.26 MW. The EV battery capacity limits are $SOE^{\text{T0}} = 0.6$, $SOE^{\text{MAX}} = 1$, $SOE^{\text{MIN}} = 0.2$.

C. Characteristic Days

The models are tested on four characteristic days:

- Day 1 – energy price curve with low daily volatility and low FCR capacity price,
- Day 2 – energy price curve with low daily volatility and high FCR capacity price,
- Day 3 – energy price curve with high daily volatility and low FCR capacity price,
- Day 4 – energy price curve with high daily volatility and high FCR capacity price.

The prices are taken from the EPEX and from the RTE website for 2018-2019. The aFRR is the same in all four days as its price in France is regulated.

IV. RESULTS AND DISCUSSION

The relevant results are shown as time-series in Figures 2–4 for Day 1 and as aggregates in Table II for the four characteristic days. They are based on the ex-post simulation using 100 scenarios, each corresponding to a timeseries of the RA ratios. If the reserve is scheduled in the DA, it affects the SOE of a particular EV. If the RA at a certain time-step is such that it steers the SOE to its limits and disables the adherence of the planned DA schedule, the aggregator must redispatch this EV by trading in subsequent intraday/balancing markets to backtrack the SOE to its DA-planned value. The SOE limits cannot be violated as any kind of charging or discharging would stop if an EV reaches the battery limits. However, in this ex-post analysis the violation of the SOE limits is used as an indicator if the EV DA scheduling algorithm incorrectly models the RA uncertainty. The goal of the proposed algorithms is to ensure that even without trading in subsequent markets the RA do not cause infeasible SOE levels.

A. Day-ahead Plans – Day 1

Figures 2–4 show the results of the three models. Subfigures to the left show the DA schedules and subfigures to the right show how those plans affect the SOE constraints of the EV fleet. The DM schedules the maximum aFRR (at higher price as compared to the FCR) in both directions plus it schedules a lot of DA charging energy to compensate for the missing

energy. Due to a high amount of the scheduled reserves, a high number of EVs end up with their SOE limits violated in both directions (up to 581) and by a significant margin (up to -164% and 210%). In Figure 2b) the solid lines denote SOE in % and the dashed lines represent the number of EVs outside the limits in the worst scenario *Max* and excluding the 10% of the worst scenarios *Q10*.

The SM adjusts the reserve schedule to its ex-ante scenarios and results in variable reserve schedules where both the FCR and the aFRR are utilized in both directions, as shown in Figure 3. The down reserve is scheduled more frequently to avoid charging in the DA energy market. Even though the aFRR reserve is better priced, the FCR is scheduled more since it is less stochastic. Number of EVs beneath the SOE^{MIN} level is negligible during the entire day, whereas during the daytime certain amount of EVs can surpass SOE^{MAX} (up to 71 EVs and up to 155% of SOE).

The RM adjust the reserve schedule to find a trade-off between the OF and the worst-case RA. It schedules the reserve rather uniformly through the day and selects only one aFRR in down direction (higher price than FCR), as presented in Figure 4. DA energy charging and discharging is utilized to create the optimal working point for each EV, i.e. to maximize reserve provision for the worst-case realization. There is almost no EVs significantly surpassing SOE^{MAX} . The morning peak of such EVs is visible in Figure 4b), but their SOE is only slightly above SOE^{MAX} (110% as compared to 155% for the SM and 210% for the DM). None of the EVs have an SOE beneath SOE^{MIN} for the RM versus a negligible number for the SM (8 EVs down to -8.83%) and a significant number for the DM (556 EVs down to -164%). It can be concluded that both the SM and the RM compromise between the revenue and the uncertainty but in their unique way and that EVs rarely surpass their SOE limits.

B. Summarized Results – All Days

The results shown in Table II are separated in three major segments, providing the statistics on: I) the realized costs, II) the EVs whose SOE is theoretically under SOE^{MIN} , III) the EVs whose SOE is theoretically over SOE^{MAX} . Shaded cells highlight the worst results for a specific reference day, while the best results are in bold text.

As seen in Figures 2–4, the DM provides maximum possible reserve at the expense of provision infeasibility. Thus it displays the lowest costs in segment I of Table II). *Min Cost* for the DM ranges from -2570 to -1860 €, while *Max Cost* is in between -290 and -30 €. The RM, due to its strict US on the SOE limits but loose US on the OF, provides the highest cost solution. *Min Cost* is always higher than -50 € and *Max Cost* than 340. However, the DM would suffer greatly from the penalties related to energy and reserve redispatching in the real time, whereas the RM would be mostly intact by them, i.e. it would be robust to the risks of not being able to provide the scheduled services. The SM is in between those two models, with *Min Cost* ranging from -200 to -600 € and *Max Cost* in between 90 and 310 €.

In segments II) and III) of Table II, *Min/Max* parameters refer to the worst realization of the observed parameter. In

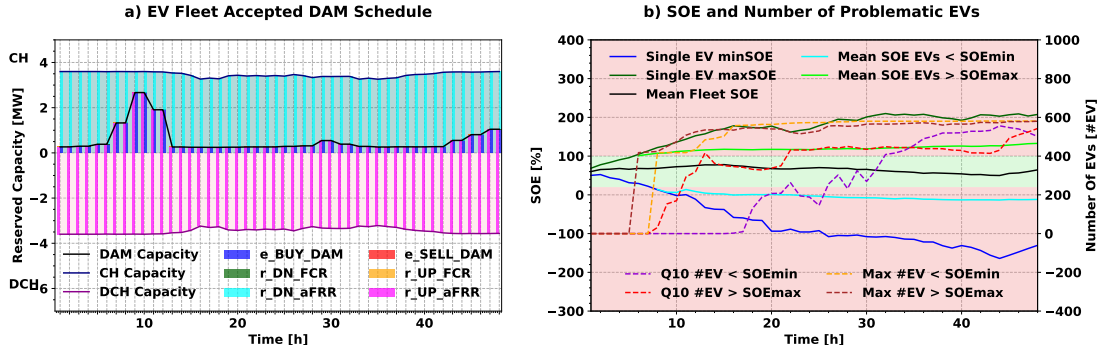


Fig. 2. Deterministic Model – Day 1

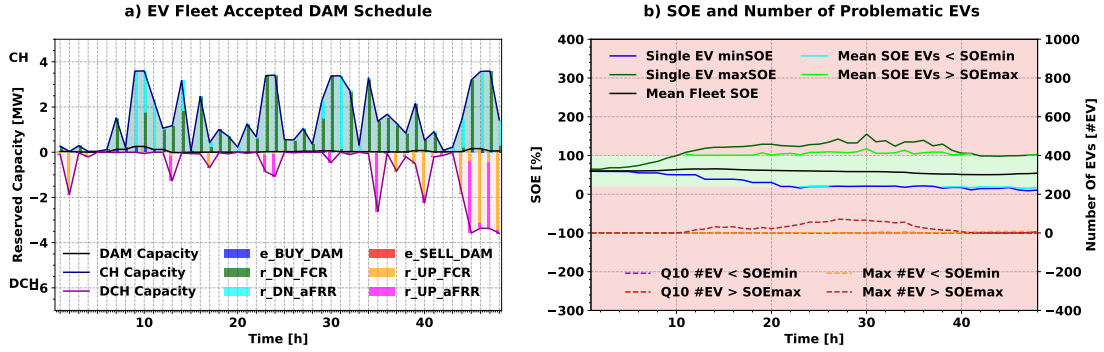


Fig. 3. Stochastic Model – Day 1

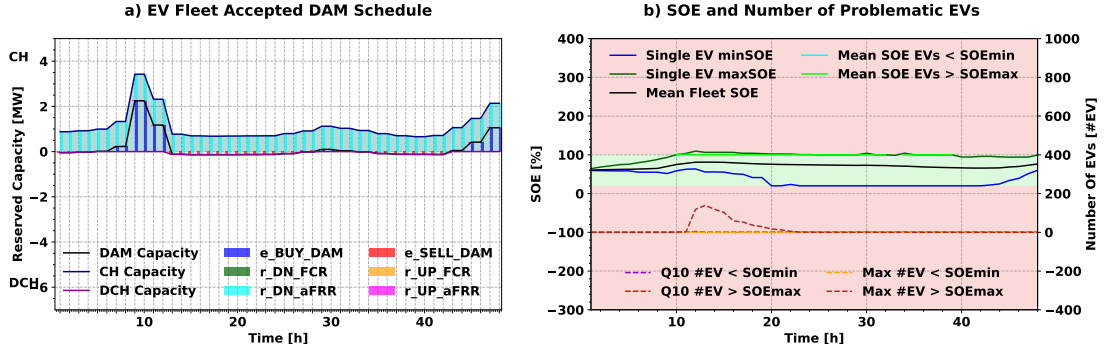


Fig. 4. Robust Model – Day 1

segment II), $Min SOE$ corresponds to the lowest EV SOE realized in the ex-post analysis. The lowest $Min SOE$ is always achieved for the DM with -164.11% in the worst characteristic day (Day 1). The SM yields better results as compared to the DM, but $Min SOE$ is still underneath the allowable limits of 20% (for the worst reference day – Day 4 it is 4.76%). The lowest SOE in the RM is just at the lower SOE limit, i.e. 20%, meaning it does not violate the SOE^{MIN} limit in any of the

observed reference days. $Max \Sigma < SOE$ indicates the overall energy below SOE^{MIN} for the entire fleet in one time-step. The DM results in highest energy mismatch, going as high as 25 MWh of unsupplied energy, the SM is in range of several dozens kWh, and the RM is without such energy mismatch. $Max \#EV <$ indicates the number of EVs with SOE falls below SOE^{MIN} in the worst case. In the DM, all or almost all EVs (520-581) suffer from the SOE lower than SOE^{MIN} . The SM

TABLE II
AGGREGATE RESULTS FOR TWO REFERENCE DAYS BASED ON 100 EX-POST SCENARIOS SIMULATION

Observed Results	Day 1			Day 2			Day 3			Day 4		
	DM	SM	RM	DM	SM	RM	DM	SM	RM	DM	SM	RM
I) Min Cost [10 ³ €]	-2.51	-0.20	0.01	-1.86	-0.59	-0.05	-2.57	-0.21	0.04	-1.87	-0.60	-0.03
Max Cost [10 ³ €]	-0.07	0.28	0.34	-0.29	0.09	0.38	-0.03	0.31	0.34	-0.29	0.12	0.37
II) Min SOE [%]	-164.11	8.83	20.00	-37.78	4.99	20.00	-141.48	6.70	20.00	-36.81	4.76	20.00
Max $\Sigma SOE <$ [MWh]	25.12	0.01	0.00	4.34	0.02	0.00	23.97	0.01	0.00	3.98	0.03	0.00
Max #EV < [#]	581	8	0	523	21	0	581	7	0	520	26	0
III) Max SOE [%]	209.89	154.97	109.60	190.26	176.93	106.84	213.27	149.01	111.78	188.53	181.31	109.37
Max $\Sigma SOE >$ [MWh]	16.15	0.27	0.15	12.95	0.50	0.31	16.15	0.36	0.22	12.41	0.60	0.10
Max #EV > [#]	580	71	139	572	307	420	580	89	170	570	457	105

schedule results in up to 26 EVs below SOE^{MIN} , whereas the RM model does not suffer from such issues.

The parameters from segment III) in Table II are analogous to those from segment II), except they refer to the EVs' upper SOE limits. $Max\ SOE$ is the highest for the DM (up to 213.27%), closely followed by the SM (up to 181.31%), and by far the lowest for the RM (up to 111.78%). High $Max\ \Sigma > SOE$ values are achieved for the DM (up to 16.15 MWh), whereas the SM and RM are in the range of several hundreds kWh (RM lower for all characteristic days). Maximum number of EVs above SOE^{MAX} ($Max\ \#EV >$) is extremely high for the DM (almost all EVs, 570-580), but also relatively high for the SM and RM as well (up to 457 and 420, respectively). For the first three characteristic days the SM even achieves better results than the RM. However, these numbers should be observed in relation to the maximum value of SOE. The high number of EVs above SOE^{MAX} for the RM means high number of EVs whose SOE is just slightly above SOE^{MAX} .

To conclude this results analysis, from the perspective of the SOE limits violation, the RM provides the best solution closely followed by the SM. The DM is prone to high deviations in actual realization of RA.

V. CONCLUSION

The paper brings a novel approach to modelling uncertainty within scheduling of automatic reserves activation (both aFRR and FCR) in European markets. It proposes stochastic- and robust-based optimization models, where scenarios and uncertainty sets are based on an analysis of real-world historical data. The existing deterministic model fails to properly accommodate the uncertain aspects of the reserve activation. The presented case study clearly demonstrates the advantages of the proposed approaches.

Although claiming high DA benefits, the deterministic model results in extreme individual violations of the EVs' battery SOE limits, ranging from -160% to above 200% SOE. Additionally, it results in high fleet-level deviations, from 25 MWh above SOE^{MAX} to 15 MWh below SOE^{MIN} . These deviations would, in reality, manifest as an inability to provide the scheduled DA energy, activated reserve energy or driving energy. The stochastic and robust formulations decrease the risks related to infeasible reserve activations. Minimum and maximum individual SOE levels achieved in the stochastic model are 4.76% and 181.31% of SOE and in the robust model 20% and 111.78% SOE. At the fleet level, energy levels below SOE^{MIN} are negligible, while levels above SOE^{MAX} are in the range of dozens of kWh. Both formulations are technology-agnostic and can be implemented in other algorithms (redispatch measures, other markets, adaptive robust algorithms, etc.) and paired with price, behavior or bid acceptance uncertainties. However, the robust model is more flexible and there are many improvements to be made on top of the the features presented in this paper, e.g. it can be further tailored for specific needs tightening or relaxing specific US parameters.

REFERENCES

[1] International Energy Agency, "Global EV Outlook 2019," Technical Report, 2019.

[2] International Renewable Energy Agency, Innovation landscape brief: Electric-vehicle smart charging, Technical Report, 2019.

[3] G. Pasaoglu, D. Fiorello, A. Martino, G. Scarcella, A. Alemanno, A. Zubaryeva, and C. Thiel, "Driving and parking patterns of European car drivers - a mobility survey," European Commission Report, 2012.

[4] ENTSO-E, "ENTSO-E Balancing Report," 2020.

[5] ACER, "ACER Market Monitoring Report 2019 – Electricity Wholesale Markets Volume," ACER Market Monitoring Report 2018 – Electricity Wholesale Markets Volume, 2019.

[6] J. Figgenger *et al.*, "The development of stationary battery storage systems in Germany — A market review," *J. Energy Storage*, vol. 29, p. 101153, Jun. 2020.

[7] Ramboll, "Ancillary Services From New Technologies," Technical Report, 2019.

[8] J. Engels, "Integration of Flexibility from Battery Storage in the Electricity Market," PhD Thesis, 2020.

[9] M. Alipour *et al.*, "Stochastic scheduling of aggregators of plug-in electric vehicles for participation in energy and ancillary service markets," *Energy*, vol. 118, pp. 1168–1179, Jan. 2017.

[10] M. Shafie-Khah, M. P. Moghaddam, M. K. Sheikh-El-Eslami, and J. P. S. Catalao, "Optimised performance of a plug-in electric vehicle aggregator in energy and reserve markets," *Energy Convers. Manag.*, vol. 97, pp. 393–408, Jun. 2015.

[11] I. Momber *et al.*, "Risk averse scheduling by a PEV aggregator under uncertainty," *IEEE Trans. Power Syst.*, vol. 30, no. 2, pp. 882–891, Mar. 2015.

[12] S. I. Vagropoulos and A. G. Bakirtzis, "Optimal bidding strategy for electric vehicle aggregators in electricity markets," *IEEE Trans. Power Syst.*, vol. 28, no. 4, pp. 4031–4041, 2013.

[13] P. Sanchez-Martin, S. Lumberras, and A. Alberdi-Alen, "Stochastic programming applied to ev charging points for energy and reserve service markets," *IEEE Trans. Power Syst.*, vol. 31, no. 1, pp. 198–205, Jan. 2016.

[14] R. J. Bessa and M. A. Matos, "Optimization models for EV aggregator participation in a manual reserve market," *IEEE Trans. Power Syst.*, vol. 28, no. 3, pp. 3085–3095, 2013.

[15] C. Goebel and H. A. Jacobsen, "Aggregator-Controlled EV Charging in Pay-as-Bid Reserve Markets with Strict Delivery Constraints," *IEEE Trans. Power Syst.*, vol. 31, no. 6, pp. 4447–4461, Nov. 2016.

[16] P. Hasanpor Divshali and C. Evens, "Optimum Operation of Battery Storage System in Frequency Containment Reserves Markets," *IEEE Trans. Smart Grid*, vol. 11, no. 6, pp. 4906–4915, Nov. 2020.

[17] M. Merten *et al.*, "Bidding strategy for battery storage systems in the secondary control reserve market," *Appl. Energy*, vol. 268, p. 114951, 2020.

[18] K. Pandžić, I. Pavić, I. Andročec, and H. Pandžić, "Optimal Battery Storage Participation in European Energy and Reserves Markets," *Energies*, 2020.

[19] G. Liu, Y. Xu, and K. Tomovic, "Bidding strategy for microgrid in day-ahead market based on hybrid stochastic/robust optimization," *IEEE Trans. Smart Grid*, vol. 7, no. 1, pp. 227–237, Jan. 2016.

[20] M. Kazemi *et al.*, "Operation Scheduling of Battery Storage Systems in Joint Energy and Ancillary Services Markets," *IEEE Trans. Sust. Energy*, vol. 8, no. 4, pp. 1726–1735, Oct. 2017.

[21] M. R. Sarker, Y. Dvorkin, and M. A. Ortega-Vazquez, "Optimal participation of an electric vehicle aggregator in day-ahead energy and reserve markets," *IEEE Trans. Power Syst.*, vol. 31, no. 5, pp. 3506–3515, Sept. 2016.

[22] I. Pavić, H. Pandžić, T. Capuder, "Electric Vehicles as Frequency Containment Reserve Providers," in *Proceedings of IEEE International Energy Conference (ENERGYCON)*, Gammarth, Tunisia, Oct. 2020.

[23] B. Han *et al.*, "Day-ahead electric vehicle aggregator bidding strategy using stochastic programming in an uncertain reserve market," *IET Gener. Transm. Distrib.*, vol. 13, no. 12, pp. 2517–2525, Jun. 2019.

[24] M. A. Ortega-Vazquez, "Optimal scheduling of electric vehicle charging and vehicle-to-grid services at household level including battery degradation and price uncertainty," *IET Gener. Transm. Distrib.*, vol. 8, no. 6, pp. 1007–1016, June 2014.

[25] RTE, "RTE Customer's area - Volumes and prices." [Online]. Available: <https://clients.rte-france.com> [Accessed: 22-Jan-2019].

[26] C. Thiel, A. Alemanno, G. Scarcella, A. Zubaryeva, and G. Pasaoglu, "Attitude of European car drivers towards electric vehicles: a survey," JRC Report, 2012.

[27] G. Pasaoglu *et al.*, "Projections for EV Load Profiles in Europe Based on Travel Survey Data Contact information," JRC Report, 2013.

[28] J. M. Morales *et al.*, *Integrating Renewables in Electricity Markets*, vol. 205. Boston, MA: Springer US, 2014.